

Competing exchange interactions in Co-doped ZnO: Departure from the superexchange picture

S. D'Ambrosio,¹ V. Pashchenko,² J.-M. Mignot,³ O. Ignatchik,⁴ R. O. Kuzian,⁵ A. Savoyant,¹ Z. Golacki,⁶
K. Graszka,⁶ and A. Stepanov^{1,*}

¹IM2NP, CNRS UMR 6242, FST, Aix-Marseille Université, F-13397 Marseille Cedex 20, France

²B. I. Verkin Institute for Low Temperature Physics and Engineering, National Academy of Sciences of Ukraine, 61103 Kharkov, Ukraine

³Laboratoire Léon Brillouin, CEA/Saclay, CEA-CNRS, F-91191 Gif sur Yvette, France

⁴Hochfeld-Magnetlabor Dresden, Helmholtz-Zentrum Dresden-Rossendorf, D-01314 Dresden, Germany

⁵Institute for Materials Science, Krzhizhanovskogo 3, 03180, Kiev, Ukraine

⁶Institute of Physics, Polish Academy of Sciences, Al. Lotnikow 32/46, 02-668, Warsaw, Poland

(Received 28 December 2011; published 5 July 2012)

We report the results of a comprehensive study of the exchange interactions in Co-doped ZnO using inelastic neutron scattering, electron paramagnetic resonance, and magnetic property measurements. In particular, we observe an unprecedentedly strong spatial anisotropy of the two nearest-neighbor exchanges, $J^{(1)} = -25.6 \pm 0.3$ K and $J^{(2)} = -8.5 \pm 0.4$ K, along with the distant-neighbor J values of ferromagnetic sign. We argue that the superexchange mechanism alone cannot account for the obtained data and we suggest that an additional mechanism leading to a strong ferromagnetic spin coupling is responsible for these findings. We also discuss the origin of this ferromagnetic mechanism.

DOI: [10.1103/PhysRevB.86.035202](https://doi.org/10.1103/PhysRevB.86.035202)

PACS number(s): 75.50.Pp, 75.30.Et, 75.50.Ee

I. INTRODUCTION

The discovery of ferromagnetism in diluted magnetic semiconductors (DMSs) has triggered intensive studies aimed at understanding the underlying mechanisms behind the spin-spin interactions in these materials.¹⁻⁴ It is still a great challenge to develop a ferromagnetic (FM) semiconductor with a critical temperature (T_c) well above room temperature. While various models have been proposed to explain T_c in DMSs, most of them consider the observed ferromagnetism as a result of competition between FM Zener exchange interaction and antiferromagnetic (AFM) superexchange (SE).⁵ Clearly, both of them are of fundamental importance in establishment of the ordered state. The SE mechanism is the focus of the work reported here.

The situation with undoped DMSs seemed to be fairly well understood: according to the SE model, their magnetic properties are dominated by AFM interactions.⁶ This general statement is expected to be valid for both nearest-neighbor (NN) exchange parameters and distant-neighbor (DN) ones.

Larson *et al.* were the first who worked out an SE model for the NN exchange, J_1 , in zinc-blende alloys.⁷ In *wurtzite materials*, in contrast with zinc-blende ones, one needs two NN J values, which are denoted J_1^{in} and J_1^{out} . This raises an interesting question about the spatial anisotropy of J_1 's, which can be parameterized by $\xi = \Delta J_1 / J_1$ ($\Delta J_1 = J_1^{\text{in}} - J_1^{\text{out}}$, $J_1 = (J_1^{\text{in}} + J_1^{\text{out}}) / 2$).^{8,9} Currently available data reveal that ξ is strongly material dependent but does not exceed a few tenths: $\xi \simeq 0.13, 0.15, 0.29$, and 0.19 for CdS:Mn, CdSe:Mn, ZnO:Mn, and CdS:Co, respectively.^{8,10} Most recently⁹ it was pointed out that the experimental data on ξ offer a crucial test of the validity of the SE model, since ξ , in contrast to the J values, does not depend on the choice of the electronic structure parameters (for details, see below).

The DN exchange constants, J_n (where $n = 2$ for second neighbors, $n = 3$ for third neighbors, etc.), provide rare, if not unique, information about the distance dependence of hybridization processes in DMSs.¹¹ According to the

theoretical models, the J_n are all AFM and rapidly decrease with n ($J_n \sim r_n^{-\alpha}$, where $\alpha \simeq 7 \div 9$ and r_n is the distance between DN's¹²⁻¹⁴). These predictions are supported by numerous studies employing magnetization step experiments⁸ and inelastic neutron scattering (INS) measurements.¹⁵ Note, however, that (i) the majority of available data were obtained on Mn-doped DMSs (including wide-gap materials);¹⁰ (ii) to the best of our knowledge, all investigations reported so far are limited by the observation of four or five largest AFM exchange constants; and (iii) the magnetization step method, due to its methodological constraints, has difficulties in probing FM exchange constants. Nevertheless, the up-to-date data available do not reveal any deficiency of SE model in DMSs.

In this paper we present the first clear evidence of a departure from this picture. Our observations rather support the idea of the competing nature of the exchange interactions in ZnO:Co, which are built up of FM and AFM contributions. Experimentally this manifests itself in two ways: we observe an unusually large spatial anisotropy of NN exchange constants, $\xi \simeq 1$, $J^{(1)} = -25.6 \pm 0.3$ K, and $J^{(2)} = -8.5 \pm 0.4$ K, along with the DN J values of FM sign. To explain these findings, we propose a model which suggests that the SE mechanism alone cannot account for the obtained data and that direct p - d FM exchange interactions play a role in determining the exchange constants of ZnO:Co.

II. EXPERIMENTAL RESULTS

We start the presentation of our experimental results by discussing the INS experiments. The experiments were performed on powder samples of $\text{Zn}_{0.97}\text{Co}_{0.03}\text{O}$, in the temperature range 1.5–100 K, using cold neutron triple-axis spectrometer 4F2 at Laboratoire Léon Brillouin (Saclay). The spectrometer is equipped with a double pyrolytic graphite monochromator, providing wavelengths between 6 and 2 Å ($1.05 < k_i < 3.2$ Å⁻¹). The incident beam was filtered by a N_2 -cooled Be filter. In addition, a 4-cm-thick pyrolytic graphite filter was

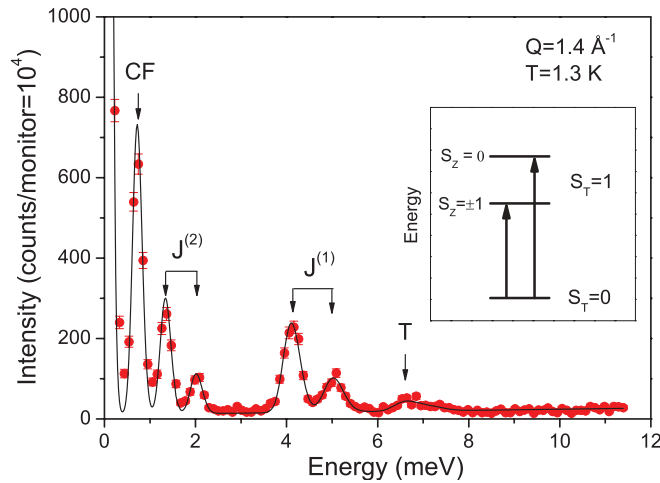


FIG. 1. (Color online) Inelastic-neutron-scattering spectrum of a $\text{Zn}_{0.97}\text{Co}_{0.03}\text{O}$ powder sample for $Q = 1.4 \text{ \AA}^{-1}$ at $T = 1.3 \text{ K}$; the line is the fit by Gaussian peaks. Inset: Schematic of the low-energy part of the Co^{2+} pair spectrum when $|J| \gg D$.

used in the scattered beam to reduce higher order contributions. Pyrolytic graphite (002) reflection planes were used for both the monochromator and the analyzer, with the monochromator being vertically focused and the analyzer flat or horizontally focused. All measurements were done with a fixed final wave vector.

In Fig. 1 we show the INS spectrum of a $\text{Zn}_{0.97}\text{Co}_{0.03}\text{O}$ powder sample for $Q = 1.4 \text{ \AA}^{-1}$ at $T = 1.3 \text{ K}$. An important point is that the positions of all observed peaks do not depend, within the experimental error, on the momentum transfer, which was varied in the range of $0.95 < Q < 3.0 \text{ \AA}^{-1}$. This provides clear evidence in favor of an isolated-cluster origin of the observed excitations. In fact, a strong maximum at 0.68 meV (labeled CF in Fig. 1) is due to the transition in Co^{2+} singles between $|\pm 1/2\rangle$ and $|\pm 3/2\rangle$ states of $S = 3/2$ ¹⁶ and a broad feature at about 6.7 meV (labeled T) can be tentatively attributed to NN closed triplets of Co^{2+} . We assume that the remaining four peaks come from NN Co^{2+} pairs. In order to identify them and to extract the NN exchange parameters, we use a simple spin Hamiltonian model describing an isolated Co^{2+} pair, which includes the exchange interaction $H_{\text{ex}} = -2J \vec{S}_1 \cdot \vec{S}_2$ and the single-ion anisotropy term $D(S_i^z)^2$ with $D = 0.342 \text{ meV}$.¹⁶ The energy levels of an AFM pair is labeled by the total spin $\vec{S}_T = \vec{S}_1 + \vec{S}_2$ (where $S_T = 0, 1, 2, 3$), provided that $|J| \gg D$. Note that, according to this model, the first excited state $|S_T = 1\rangle$, which is separated by $\sim 2|J|$ from the $|S_T = 0\rangle$ state, is further split by $\sim 2.4D$ (see the inset in Fig. 1). Now, because in INS processes the allowed transitions require $\Delta S_T = 0, \pm 1$,¹⁷ one should observe, at low temperatures, a *double-peak structure* corresponding to each particular type of NN pairs of Co^{2+} , with approximately equal integral intensities, because the coordination numbers for both the in-plane and the out-of plane NN pairs are identical, $z_n = 6$ [hereafter, we use the classification of neighbors in the wurtzite structure given in Ref. 10 (see their Table I), along with the definitions of z_n and $J(n)$]. If one takes into account that the experiments were performed with unpolarized neutrons and that D is positive in ZnO:Co , the transition

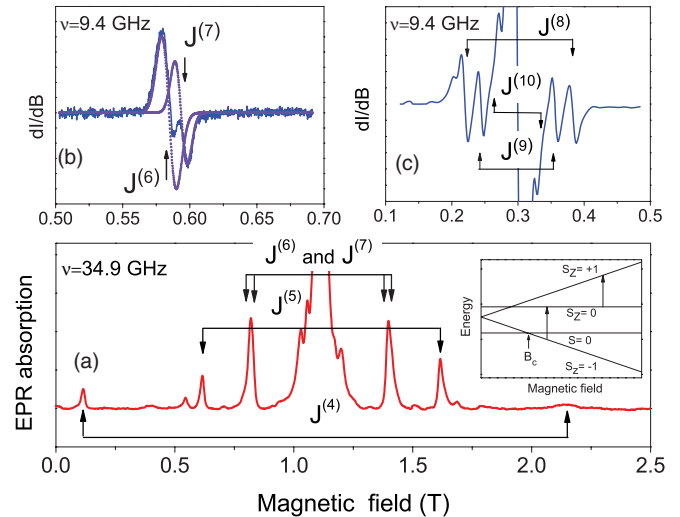


FIG. 2. (Color online) EPR spectra of $\text{Zn}_{1-x}\text{Co}_x\text{O}$ single crystals for $B||c$. (a) For $x = 0.02$, $\nu = 34.9 \text{ GHz}$, and $T = 1.5 \text{ K}$. Arrows indicate the positions of Co^{2+} pair satellites. Inset: Energy-field diagram of a Co^{2+} pair for $D \gg |J|$. Arrows represent the observed intertriplet transitions; the energy-level crossing field B_c is also shown. (b) Part of the X-band spectrum for $x = 0.001$ taken at 4 K which presents contributions from $J^{(6)}$ and $J^{(7)}$ pairs. (c) Part of the X-band spectrum for $x = 0.02$ at 4 K which shows contributions from $J^{(8)}$, $J^{(9)}$, and $J^{(10)}$ pairs.

$|S_T = 0\rangle \rightarrow |S_z = \pm 1\rangle$ must be lower in energy than the transition $|S_T = 0\rangle \rightarrow |S_z = 0\rangle$, and the intensity of the former transition must be twice as large as that of the latter. Based on the above arguments, we attribute the double-peak structures at $4.1/5.0$ and at $1.4/2.0 \text{ meV}$ to NN Co^{2+} pairs coupled by the two largest exchange constants, $J^{(1)} = -25.6 \pm 0.3 \text{ K}$ and $J^{(2)} = -8.5 \pm 0.4 \text{ K}$, respectively.

To proceed with the determination of DN exchange constants we use the electron paramagnetic resonance (EPR) technique at helium temperatures, in the frequency range from 9.4 to 90 GHz and in a magnetic field up to 6 T . A few single crystals of $\text{Zn}_{1-x}\text{Co}_x\text{O}$ with $0.001 < x < 0.02$ were used. The EPR spectrum ($h\nu \ll D$) of an isolated Co^{2+} in the ZnO lattice is well known and well understood. When a magnetic field B is applied parallel to the crystallographic c axis, a single line with $g_{\parallel} = 2.236$ is observed, which is due to the low-lying doublet $|\pm 1/2\rangle$ of an $S = 3/2$ ground-state manifold.¹⁶ At low temperatures, $T \ll D/k$, the EPR spectra of Co^{2+} pairs show up as weak satellites to this main line, resulting from the four lowest energy levels of a Co^{2+} pair. We describe these levels by an effective spin $S = 0$ (a quasisinglet state) and $S = 1$ (a quasitriplet state) using the above-described spin Hamiltonian. The energy-field diagram in Fig. 2(a) illustrates this for an AFM coupled pair of Co^{2+} . Because the transition between $|S = 0\rangle$ and $|S = 1\rangle$ states is forbidden, it is easy to see that, for a given J , if the EPR frequency exceeds $\nu \approx (3|J| + 10J^2/D)/h$, one can observe both allowed intertriplet transitions, $|-1\rangle \rightarrow |0\rangle$ and $|0\rangle \rightarrow |+1\rangle$, which are equally spaced with respect to the main EPR line.

In Fig. 2(a) a representative EPR spectrum for a $\text{Zn}_{0.98}\text{Co}_{0.02}\text{O}$ single crystal, taken at $\nu = 34.9 \text{ GHz}$, is shown, on which satellite lines originating from various Co^{2+} pairs

TABLE I. Experimentally obtained exchange parameters of Co^{2+} pairs in $\text{ZnO}:\text{Co}$ and their coordination numbers.

	Exchange parameter (K)	Coordination number
$J^{(1)}$	-25.6 ± 0.3	6
$J^{(2)}$	-8.5 ± 0.4	6
$J^{(3)}$	-1.070 ± 0.003	2
$J^{(4)}$	-0.382 ± 0.002	6
$J^{(5)}$	0.347 ± 0.002	6
$J^{(6)}$	0.168 ± 0.002	12
$J^{(7)}$	-0.134 ± 0.002	6
$J^{(8)}$	-0.040 ± 0.001	6
$J^{(9)}$	-0.027 ± 0.001	12
$ J^{(10)} $	0.013 ± 0.001	12

are clearly seen, as well as the main line at $B = 1.11$ T. The difference in the resonance fields of two satellites belonging to the same $J^{(n)}$ enables one to calculate the corresponding $J^{(n)}$. Their relative intensity at a given temperature provides information about the sign of $J^{(n)}$ and its coordination number z_n . For particular values of ν and T the EPR spectra were fitted using the *easyspin* toolbox,¹⁸ thus allowing us to obtain the above-mentioned parameters. To illustrate this, we take the case of two satellites labeled $J^{(5)}$ and positioned at $B = 0.615$ T [we call this the low-field satellite (LFS)] and at $B = 1.615$ T [called the high-field satellite (HFS)]. First, we try to simulate the observed spectra using the two distinct models for a Co^{2+} pair: an AFM coupled pair and an FM coupled one. Proceeding in this way, one can perfectly fit the observed line positions in either model, but not the line intensities. In fact, the FM model gives $J^{(5)} = 0.347 \pm 0.002$ K and predicts that the intensity of the LFS, I_{LFS} , is about two times lower than the intensity of the HFS, I_{HFS} (the calculated ratio $I_{\text{LFS}}/I_{\text{HFS}}$ is found to be 0.47), in good agreement with the experiment [see Fig. 2(a)]. Contrary to this, the AFM model gives $I_{\text{LFS}} > I_{\text{HFS}}$ with $I_{\text{LFS}}/I_{\text{HFS}} \simeq 4$. One may, therefore, safely conclude that the Co^{2+} ions in $J^{(5)}$ pairs are coupled *ferromagnetically*. This conclusion is then supported by an analysis of other EPR spectra measured at various temperatures and frequencies. In a similar way it can be shown that $J^{(4)}$ satellites are due to AFM coupled Co^{2+} pairs with $J^{(4)} = -0.382 \pm 0.002$ K, and their coordination number, $z_n(J^{(4)})$, is very close to that of $J^{(5)}$ pairs.

The situation with two satellites labeled $J^{(6)}$ and $J^{(7)}$ is somewhat more complicated. A thorough examination of the EPR spectra obtained shows that each of them consists of two closely spaced EPR components with the intensity ratio $I(J^{(6)})/I(J^{(7)}) \simeq 2$ as illustrated in Fig. 2(b), where the fine structure of the HFS is shown and analyzed. The best fit to these two EPR components gives $J^{(7)} = -0.134 \pm 0.002$ K and $J^{(6)} = 0.168 \pm 0.002$ K, with $z_n(J^{(7)}) \simeq z_n(J^{(5)})$ and $z_n(J^{(6)}) \simeq 2z_n(J^{(5)})$. For completeness in Fig. 2(c) the EPR spectra of three additional Co^{2+} pairs are shown. They give rise to three extra $J^{(n)}$'s— $J^{(8)}$, $J^{(9)}$, and $J^{(10)}$ —which are only of the order of a few tens of millikelvins (see Table I). While it is clear that, at this energy scale, mechanisms other than SE may contribute to $J^{(n)}$'s, for the sake of simplicity we continue to refer to them as the exchange constants.

In addition to the pair spectra shown in Fig. 2, at frequencies higher than 60 GHz, a much weaker spectrum was observed,

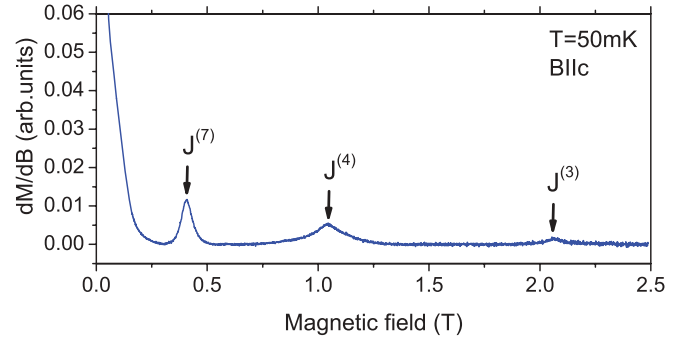


FIG. 3. (Color online) Field dependence of magnetic ac susceptibility in a $\text{Zn}_{0.98}\text{Co}_{0.02}\text{O}$ single crystal at $T = 50$ mK.

which is characterized by an energy gap of 106.5 GHz between the $|S_z = \pm 1\rangle$ and the $|S_z = 0\rangle$ states at $B = 0$. We attribute this spectrum to AFM Co^{2+} pairs coupled by the third largest exchange constant, $J^{(3)} = -1.07 \pm 0.003$ K. Since we have not succeeded in the determination of the coordination number of these $J^{(3)}$ pairs in the EPR experiment, we have undertaken ac susceptibility measurements at subkelvin temperatures.

In Fig. 3 the field dependence of magnetic ac susceptibility, dM/dB (where M is the magnetization), measured on a $\text{Zn}_{0.98}\text{Co}_{0.02}\text{O}$ single crystal at $T = 50$ mK is shown. Three peaks of dM/dB , which are clearly shown at $B = 0.41$, 1.05, and 2.07 T, result from the energy-level crossing, at B_c , of the $|S_z = -1\rangle$ triplet state with the $|S = 0\rangle$ one of the corresponding Co^{2+} pair [see the inset in Fig. 2(a)]. No other signal which can be associated with the magnetization step was observed up to 6 T. By comparing the B_c estimated from the exchange constants obtained by EPR— $B_c(J^{(7)}) = 0.41$ T, $B_c(J^{(4)}) = 1.02$ T, and $B_c(J^{(3)}) = 1.91$ T—with the measured ones, we attribute these ac susceptibility peaks to the three AFM coupled pairs $J^{(7)}$, $J^{(4)}$, and $J^{(3)}$, respectively. Most importantly, comparison of the integral intensity of the observed peaks, $I(J^{(7)}) \simeq I(J^{(4)})$ and $I(J^{(4)}) \simeq 3I(J^{(3)})$, allows one to conclude that the coordination numbers $z_n(J^{(4)}) \simeq z_n(J^{(7)})$ and $z_n(J^{(4)}) \simeq 3z_n(J^{(3)})$. These findings are decisive in identification of the DN J values. A summary of our results is given in Table I, where the values and coordination numbers for the 10 largest exchange constants obtained by INS and EPR, are listed in order of their decreasing strength. Note that the DN J values exhibit sign changes, in significant disagreement with the existing theory.

III. DISCUSSION

We turn now to calculations of the exchange parameters in $\text{ZnO}:\text{Co}$ by adapting an SE model proposed by some of us for estimation of the J values in Mn-doped wurtzite DMSs.⁹ This model is based on the p - d hybridization scheme, which is widely employed for the interpretation of photoemission data, therefore, we use the electronic structure parameters of $\text{ZnO}:\text{Co}$ obtained in the photoemission experiments: $U = 6 \pm 0.5$ eV, $\Delta = 5 \pm 0.5$ eV, and $(pd\sigma) = -1.6 \pm 0.1$ eV.¹⁹

Using these photoemission data we get two quite different NN J values, $J_1^{\text{in}} \simeq -25.1$ K and $J_1^{\text{out}} \simeq -14.6$ K, as well as the four largest DN exchanges, which are proved to be all negative (AFM).²⁰ Note that the latter result is in agreement

with the previous calculations made in the framework of the SE model but is in significant disagreement with our experimental observations. The results regarding the J_1 's allow us to assign the two largest exchange integrals in ZnO:Co by associating the observed $J^{(1)}$ and $J^{(2)}$ with the calculated J_1^{in} and J_1^{out} , respectively. Remaining unsolved, however, is the noticeable discrepancy between the theoretical and the experimental values of J_1^{out} .

To understand its origin, it is much more instructive to consider the dimensionless parameter ξ , instead of the absolute value of J_1 's. The advantage is that ξ , in contrast to J_1 , does not depend on the choice of the electronic structure parameters.⁹ It depends, however, on the choice of $(pd\sigma)(R)$, the distance dependence of the transfer integral. Therefore, to reduce the difference between the experimentally observed value, $\xi \simeq 1$, and the calculated value, $\xi = 0.52$, we first tried to replace $(pd\sigma)(R) \sim 1/R^{3.5}$, used in the present model, with $(pd\sigma)(R) \sim 1/R^4$.¹¹ This gives $\xi = 0.49$, which is even farther from the measured value than the previous one.

The second possibility for resolving this discrepancy is to introduce in the SE model an *additional FM exchange coupling between 3d electrons*. The most plausible candidate for that would be the direct p - d FM exchange K_{pd} , which is widely discussed in cuprate physics.²¹ It was shown that a hybrid process, in which the virtual hopping is combined with the direct p - d exchange leads to an extra FM contribution to the d - d exchange constant, $J^{\text{FM}} \sim K_{pd}(t_{pd}^2/\Delta^2)$, which can be as large as 50% of the total AFM contribution. Rough estimates show

that, in the case of ZnO:Co, to reproduce the experimentally observed ratio $\xi \simeq 1$, J^{FM} may amount to 35% of J_1^{in} , which seems quite reasonable.

IV. CONCLUSION

In conclusion, by combining INS, EPR, and magnetic measurements, we have performed a comprehensive study of the exchange parameters in Co-doped ZnO. Our important experimental findings are the observations of an unusually strong spatial anisotropy of the NN exchange integrals, $\xi \simeq 1$, along with the DN exchange constants of FM sign. To analyze these data we have proposed an SE model, which is in qualitative agreement with the experimental results as far as NN J values are concerned, while predicting, however, a much lower value of ξ compared to the measured one, $\xi = 0.52$. We argue that this discrepancy clearly indicates that the d - d exchange interactions in ZnO:Co are made up of competing AFM and FM contributions and that the SE mechanism alone cannot account for the obtained data.

We speculate that the introduction of this additional FM mechanism to the conventional SE model is a key point in understanding the observed sign changes of the DN exchange constants, even though, for the moment, we do not have a quantitative model for DN J values. It would be interesting to check how general our conclusion is by analyzing experimental data from magnetic, magneto-optical, and other studies which require the SE model for their interpretation.

*Corresponding author: anatoli.stepanov@im2np.fr

¹H. Ohno, *Science* **291**, 840 (2001).

²T. Dietl, H. Ohno, F. Matsukura, J. Cibert, and D. Ferrand, *Science* **287**, 1019 (2000).

³J. M. D. Coey, M. Venkatesan, and C. B. Fitzgerald, *Nat. Mater.* **4**, 173 (2005).

⁴S. Kuroda, N. Nishizawa, K. Takita, M. Mitome, Y. Bando, K. Osuch, and T. Dietl, *Nat. Mater.* **6**, 440 (2007).

⁵K. Sato, L. Bergqvist, J. Kudrnovský, P. H. Dederichs, O. Eriksson, I. Turek, B. Sanyal, G. Bouzerar, H. Katayama-Yoshida, V. A. Dinh, T. Fukushima, H. Kizaki, and R. Zeller, *Rev. Mod. Phys.* **82**, 1633 (2010).

⁶T. Dietl, *Nat. Mater.* **9**, 965 (2010).

⁷B. E. Larson, K. C. Hass, H. Ehrenreich, and A. E. Carlsson, *Phys. Rev. B* **37**, 4137 (1988).

⁸Y. Shapira and V. Bindilatti, *J. Appl. Phys.* **92**, 4155 (2002).

⁹R. O. Kuzian, A. M. Daré, A. Savoyant, S. D'Ambrosio, and A. Stepanov, *Phys. Rev. B* **84**, 165207 (2011).

¹⁰X. Gratens, V. Bindilatti, N. F. Oliveira Jr., Y. Shapira, S. Foner, Z. Golacki, and T. E. Haas, *Phys. Rev. B* **69**, 125209 (2004).

¹¹W. Harrison, *Elementary Electronic Structure* (World Scientific, Singapore, 1999).

¹²T. M. Rusin, *Phys. Rev. B* **53**, 12577 (1996).

¹³S. S. Yu and V. C. Lee, *Phys. Rev. B* **52**, 4647 (1995).

¹⁴A. Twardowski, H. J. M. Swagten, W. J. M. de Jonge, and M. Demianiuk, *Phys. Rev. B* **36**, 7013 (1987); W. J. M. de Jonge and H. J. M. Swagten, *J. Magn. Mater.* **100**, 322 (1991).

¹⁵H. Kepa, V. K. Le, C. M. Brown, M. Sawicki, J. K. Furdyna, T. M. Giebultowicz, and T. Dietl, *Phys. Rev. Lett.* **91**, 087205 (2003).

¹⁶P. Sati, R. Hayn, R. Kuzian, S. Régnier, S. Schäfer, A. Stepanov, C. Morhain, C. Deparis, M. Lügt, M. Goiran, and Z. Golacki, *Phys. Rev. Lett.* **96**, 017203 (2006).

¹⁷A. Furrer and H. U. Gudel, *J. Magn. Magn. Mater.* **14**, 256 (1979).

¹⁸S. Stoll and A. Schweiger, *J. Magn. Reson.* **178**, 42 (2006).

¹⁹M. Kobayashi, Y. Ishida, J. I. Hwang, T. Mizokawa, A. Fujimori, K. Mamiya, J. Okamoto, Y. Takeda, T. Okane, Y. Saitoh, Y. Muramatsu, A. Tanaka, H. Saeki, H. Tabata, and T. Kawai, *Phys. Rev. B* **72**, 201201 (2005).

²⁰A detailed account of these results will be published elsewhere.

²¹E. B. Stechel and D. R. Jennison, *Phys. Rev. B* **38**, 4632 (1988).